JTTEE5 13:508-514
DOI: 10.1361/10599630421406
1059-9630/$19.00 © ASM International

Peer Reviewed

Effect of Grit Blasting and Spraying Angle on the Adhesion Strength of a Plasma-Sprayed Coating

M.F. Bahbou, P. Nylén, and J. Wigren

(Submitted June 17, 2003; in revised form September 3, 2003)

A study of the effects of grit-blasting and plasma-spraying angles on the adhesion strength of an alloy (Tribaloy 800) that was plasma sprayed on a titanium-base alloy is reported. Five different spray and grit-blast angles were investigated: 45°, 55°, 65°, 75°, and 90°. The surface texture in different directions was characterized by the classic average roughness and by a fractal analysis number using a two-dimensional fractal analysis method. The grit residue was measured by an x-ray spectrometer. The study showed that the maximum adhesion strength was close to a 90° blasting and spraying angle. However, the grit residue reaches its maximum at a 75° blasting angle. From the image analysis of the interface in different directions, it was found that the nonperpendicular grit blasting produces an anisotropic surface. The fractal analysis method showed a rather good correlation with the blasting angle. However, no good correlation between the fractal number and the adhesion strength was found.

Keywords: adhesion by mechanical interlocking, fractal analysis, plasma spraying, surface roughness/morphology, titanium and alloys

1. Introduction

Thermal spray coatings can fulfill several industrial applications, such as wear, corrosion resistance, and thermal insulation. However, many of these applications remain inhibited by deposit characteristics, such as limited coating adhesion, which is strongly dependent on the surface preparation prior to thermal spraying (Ref 1).

The adhesion of thermally sprayed coatings is mainly assumed to be due to a mechanical bonding (keying) between the substrate and the coating (Ref 2). This assumption is valid when the kinetic and thermal energy of the impacting particles do not involve any melting of the substrate, which would give more chance for diffusion bonding to occur. Thermal interaction is limited due to the high cooling rate of the impinging splats (on the order of 10^6 °C/s).

With this assumption in mind, it is obvious that the substrate roughness or topography plays an important role in the bonding mechanism. Usually, an optimal surface roughness is achieved by grit blasting. Roughness numbers, such as average roughness (R_a) (the arithmetic average of the height of roughness component irregularities from the mean line measured within the sampling length) or maximum roughness (R_z) (the maximum peak-to-valley height within the sampling length), are the most common parameters that are used to characterize the surface, defined, respectively, by Eq 1 and 2:

$$R_a = \frac{1}{n}\sum_{i=1}^{n} |Z_i| \quad \text{(Eq 1)}$$

$$R_{z_{max}} = \max_{Z_i} - \min_{Z_i} \quad \text{(Eq 2)}$$

where z_i is the roughness height at a point i, and n is a given number of peaks.

These characteristic numbers usually show a good correlation with the adhesion strength (Ref 3). However, Amada and Satoh (Ref 4) found that above a certain limit the adhesion strength continues to increase while the R_a remains almost constant, especially for a nonperpendicular-blasting angle. Thus, the complex nature of the chaotic substrate topography cannot be fully characterized by conventional roughness numbers. Fractal analysis is another way to characterize the surface topography through the fractal dimension (FD) number (Ref 4-6).

This study investigated the influence of grit-blasting and plasma-spraying angle combinations on adhesive strength, which has received little attention in the literature. Furthermore, the surface roughness characteristic R_a and the fractal number are compared to evaluate their relationships to the coating adhesive strength.

2. Experimental Procedure

2.1 Materials

The substrate samples were made of a titanium alloy that is commonly used in the aerospace industry, namely, Ti-6Al-4V (AMS 4928). Eighty-eight disc-shaped samples with 25 mm diameter and 6 mm thickness were prepared. The grit media used

M.F. Bahbou, and **P. Nylén,** Department of Technology, University of Trollhättan/Uddevalla, P.O.Box 957, SE-461 29, Trollhättan, Sweden; and **J. Wigren,** Thermal Spray Department, Volvo Aero Corporation, SE-461 81 Trollhättan, Sweden. Contact e-mail: fouzi.bahbou@volvo.com.

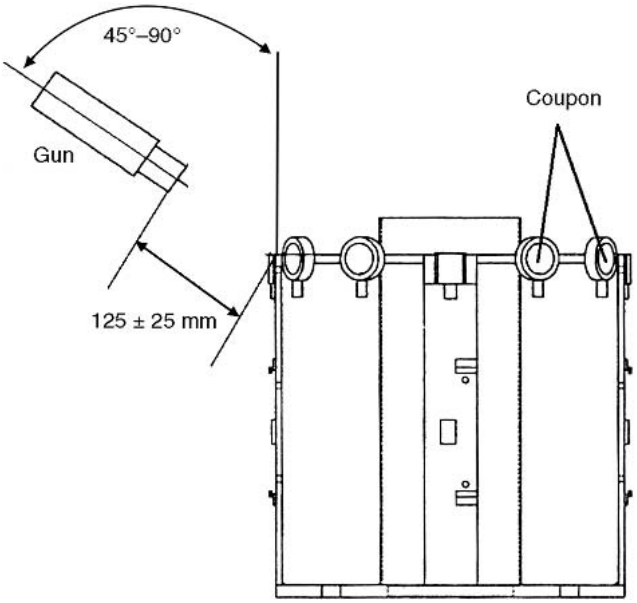

Fig. 1 Experimental fixture and setup for both grit blasting and thermal spraying

was an aluminum oxide abrasive compound with a 60-mesh size.

The plasma-sprayed coating consisted of a high-temperature wear-resistant alloy (Tribaloy 800, Volvo PM 819-15, Volvo Aero Corporation, Trollhättan, Sweden). It has a nominal composition of Co-28Mo-17Cr-3Si, in which the Co-Cr-Si is the high-temperature-resistant (up to 850 °C) hard phase and the molybdenum oxides act as lubricants. A coating thickness of about 400 μm was used to avoid any glue penetration.

2.2 Grit-Blasting and Plasma-Spraying Equipment

A suction-fed grit-blasting machine was used. The robot (ABB2000 ABB Ltd., Zurich, Switzerland)-controlled nozzle allowed a blasting angle (the angle between the sample surface and the nozzle axis) variation between 45° and 90° (Fig. 1). Plasma spraying was performed with an F4 gun (system A 3000s, Sulzer Metco, New York, NY) according to the parameters in Table 1. Five different blasting angles were evaluated (45°, 55°, 65°, 75°, and 90°). The spray angle was systematically varied within the same range as the blasting angle. To investigate whether there is a "shadowing effect," that is, when blasting nonperpendicular and spraying perpendicular. A set of samples was sprayed with the same angle used when they were blasted, and the other set was always sprayed at 90°. The assumption behind this shadowing effect is that the nonperpendicular blasting will result in peaks that have an asymmetric angle to the surface. Perpendicularly sprayed particles will not penetrate as deeply into the valleys as particles sprayed with the same angle as that used for blasting. Eight samples of each angle combination were mounted onto the fixture for statistical analysis of the scatter. In total, 11 combinations of spray and grit-blasting angles were evaluated according to the parameters in Table 2.

Table 1 Grit blasting and plasma spray parameters

Parameters	Values
Grit blasting (suction fed)	
Powder feed stock size	60 grit (0.16-0.4 mm)
Powder feed rate, kg/min	1.5
Blasting distance, mm	125
Blasting pressure, bar	4
Blasting time, s	3-4
Plasma spray (F4 spray gun)	
Arc intensity/voltage	750 A/58-68V
Spraying distance, mm	125
Argon (primary gas) flow rate, SLPM	65
H_2 (secondary gas) flow rate, SLPM	4
Carrier gas (Ar) flow rate, SLPM	3
Nozzle diameter/powder port diameter, mm	6/1.5
Powder feed rate, g/min	26 ± 2
Vertical speed/surface speed	3.5 mm/rev/75 m/min

Note: SLPM, standard liters per minute.

Table 2 Designation and repartition of samples

Sequence	Blast angle	Spray angle
1st run	45°	45°
2nd run	45°	90°
3rd run	55°	90°
4th run	65°	90°
5th run	75°	90°
6th run	90°	90°
7th run	45°	45°
8th run	55°	55°
9th run	65°	65°
10th run	75°	75°
11th run	45°	45°(a)

(a) The 45°/45° combination was repeated three times for scatter estimation.

2.3 Measurement Procedures

The R_a was measured both by a perthometer (SJ-301, Mitutoyo Corp., Kawasaki, Japan) and by image-analysis software (Aphelion, AAI, Amherst, MA; and ADCIS; Hérouville-Saint-Clair, France). The perthometer was equipped with a diamond tip of 5 μm radius. It was calibrated with a calibration surface ($R_a \approx 3$ μm) and drawn at 0.05 mm/s over a 4 mm scanned line of the grit-blasted sample. The average of ten measurements in different directions was taken (Ref 7).

The grit residues were evaluated using an x-ray analysis technique with spectrometer (Philips, Amsterdam, The Netherlands) (Ref 8). For image analysis, the samples were diamond cut, and then the coating was cold-filled with epoxy prior to hot mounting in bakelite (Ref 9). Then, the samples were ground with 120 SiC paper prior to polishing (Prepamatic machine, Struers) using a special program (Volvo Aero Corporation) that was developed for this coating system (Ref 10). The cross sections were analyzed with a microscope (PX 60M, Olympus, Tokyo, Japan) under 200× magnification. Thirty-six frames per sample interface both in the parallel and perpendicular direction to the orthogonal projection of the blasting/spraying direction on the substrate surface (for all the angles below 90°) were taken with a high-resolution CCD camera (DP 10, Olympus) and were processed by the image-analysis software. A specific procedure

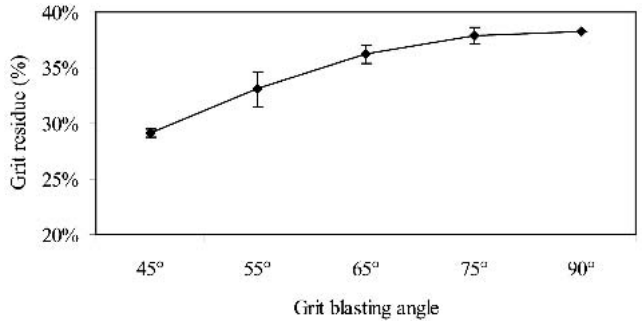

Fig. 2 Influence of blasting angle on grit residue amount (percentage by surface area)

was developed to determine the surface roughness by image analysis (image acquisition and enhancement through clarification and filtering to remove noise prior to binarization to detect the region of interest, which is the interface line). Then, the line-fit error function calculates the roughness parameter root mean square (R_q) defined as:

$$R_q = \sqrt{\sum \frac{(z_i)^2}{n}} \quad \text{(Eq 3)}$$

where z_i is the roughness height at a point i, and n a given number of peaks.

The adhesion strength of the coating was determined using a tensile testing machine (MTS 10/M, MTS Systems Corp., Eden Prairie, MN) according to the ASTM standard C 633 (Ref 11). The adhesive bonding agent used was a polytetrafluoroethylene film (FM1000, Cytec Fiberite, Winona, MN) that does not penetrate the coating upon heating and thus does not affect the adhesion strength result.

3. Results and Discussion

3.1 Grit Residue

The grit residue (given as the percentage of the surface area) increases with the blasting angle from about 30% at 45° to 38% at 90° (Fig. 2), due to the decrease in the number of the grit particles rebounding from the surface. With an increase in the angle, more particles will be embedded. This agrees well with the study carried out by Wigren (Ref 3). The error bars correspond to ±1 standard deviation (SD).

3.2 R_a Measurements

3.2.1 Perthometer Measurement. The average surface roughness increases slightly (18%) with the blasting angle from about 3.3 μm at 45° to 3.9 μm at 90°. The R_z also increases with the blasting angle from 15.5 to 24.5 μm (55%) (Fig. 3). This increase might be due to the increased plastic deformation and the cutting effect of the impinging grit particle. The error bars in Fig. 3 correspond to ±1 SD. The rather large scatter (about 1 μm) might suggest that the grit-blasted surface is not isotropic.

3.2.2 Image Analysis Measurement. As shown in Fig. 4, the R_a measured by the perthometer method and the R_q measured by the image analysis method have the same trend. However, it should be noticed that the perthometer does not take into account inner profiles (hook shapes) or profiles below the tip radius. In addition, the hard diamond tip seems to damage the surface and, thus, to underestimate the roughness. The R_a-to-R_q ratio is in the 0.8 to 0.9 range for the functions used.

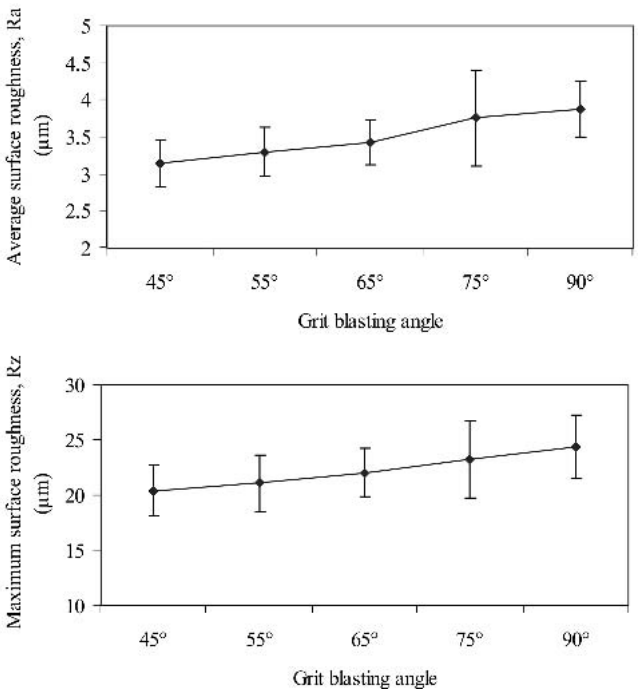

Fig. 3 Roughness numbers for different grit-blasting angles

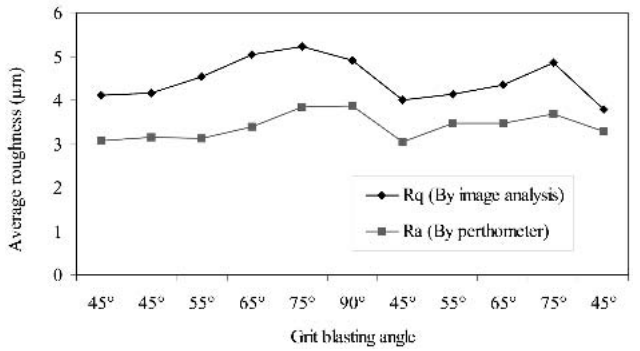

Fig. 4 Comparison between image analysis and perthometer roughness measurements

3.3 Tensile Adhesive Strength Measurements

The results of the tensile adhesive strength tests are shown in Fig. 5. The error bars correspond to ±1 SD based on 5 measurements for each angle combination and 15 measurements for the 45°/45° combination for blasting and spraying. These latter measurements were used to get a better estimation of the scatter in the results. The adhesive strength increases with the blasting angle from about 22 MPa at 45° to 28 MPa at 90° (27%) and increases even more by spraying with the same angle as the blasting angle (Fig. 5). Thus, the increase in adhesion when

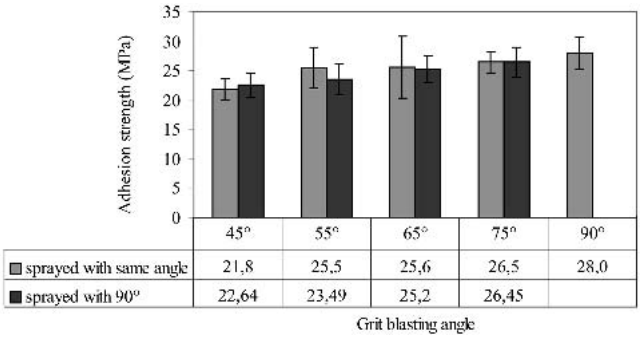

Fig. 5 Influence of grit-blasting/spraying angles on adhesion

spraying with the same angle as blasting implies that a shadowing effect exists. For instance, between 55°/90° and 55°/55° the adhesion strength increase is about 2 MPa (8.5%). However, at a 45° blasting angle this trend is not valid, which might be due to the significantly reduced impact velocity at the 45° spraying angle.

The textures of the surfaces that were blasted with different angles also were evaluated using a scanning electron microscope (SEM). Under angled blasting, one can distinguish several surface aspects (Fig. 6). At 45°, the surface texture is well developed with a lot of peaks and valleys (Fig. 6a), a condition that is favorable for adhesion (Ref 2). At 75°, the texture becomes more complicated with even more peaks and deeper valleys, thus increasing the adhesion (Fig. 6b). At a higher blasting angle (90°), the peaks seem to be flattened, forming hook-shaped profiles, which might explain the slightly higher adhesion (Fig. 6c).

A major contribution of the scatter in Fig. 5 is associated with the tensile test method because it evaluates coatings that exhibit brittle fracture, which is an unpredictable characteristic (Ref 2).

A statistical *t*-test (Ref 12) was used to determine whether the measured differences in adhesion between a blasting/spraying angle combination of 45°/90°, respectively, (the reference combination), and other combinations could be considered statistically significant or not (Table 3). The *t*-test gives the probability that the difference between the two means is caused by chance. It is customary to say that if this probability is less than 5%, then the difference is considered to be statistically significant. The *t*-test is defined as:

$$t = \frac{\text{signal}}{\text{noise}} = \frac{\text{Difference between group means}}{\text{Variability of groups}} \qquad \text{(Eq 4)}$$

By implementing the *t*-test (Eq 4) and using statistical charts, the probability of a significant difference between each two sets, assuming the null hypothesis, is found to be 1.5% with a blasting/spraying angle combination of 75°/75°, and 0.82% at 90°/90°.

3.4 Fractal Analysis

A box-counting method (Ref 4) was implemented to evaluate the FD from the determined surface profiles. The images of the coating/substrate interface were taken by a charge-coupled device (CCD) camera and processed by a binary system, and finally the interface lines corresponding to the roughened surface were obtained. These latter were covered with *N* squares of side length *L* (Fig. 7).

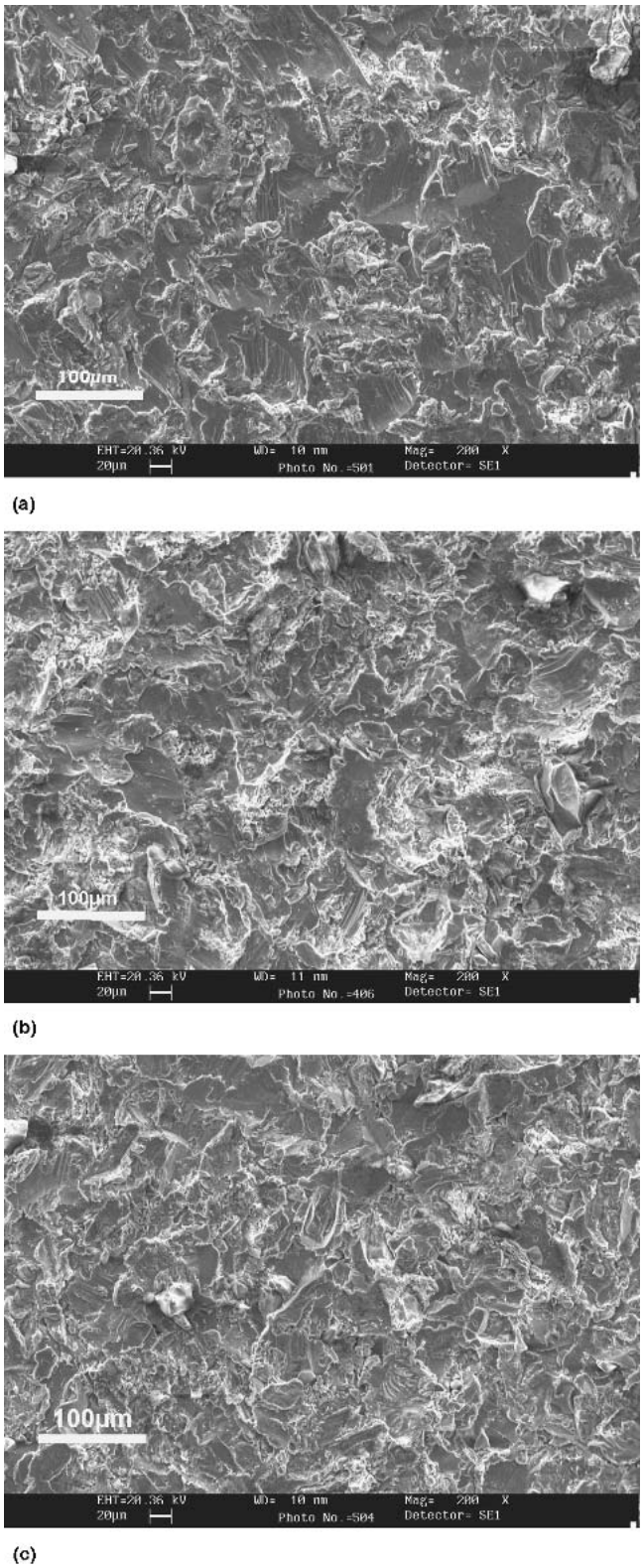

Fig. 6 Scanning electrons micrographs of grit-blasted substrates. (a) At 45°. (b) At 75°. (c) At 90°

The fractal geometry (Ref 4) gives:

$$N(L) = C \cdot L^{-D} \quad \text{(Eq 5)}$$

where D is the FD and C is a constant. By continuously varying the square size, a corresponding number of squares is obtained. These data were logarithmically plotted for each specimen profile (Fig. 8). Linear relationships between log L and log N were found. Thus, the profile had a fractal characteristic and the slope of the line was the FD. This latter increases from 0.96 at a 45° blasting and spraying angle to 1.02 at a 75° angle.

The FD of samples sprayed at the same angle that they were grit blasted is shown in Fig. 9. One set represents FD values that were computed from the substrate/coating interfaces of cross sections that were parallel to the orthogonal projection of the blasting/spraying direction on the substrate, while the second set represents the ones perpendicular to the blasting direction. The FD has a similar trend for both sets; the difference between the two sets is at a maximum with the combination blasting/spraying angle of 45°/45°, respectively. This might suggest that the blasted surface is not isotropic for low blasting angles. Figure 10 shows the resulting FD values for samples sprayed with a 90° spray angle for different blasting angles. In this case, the FD has no clear trend. The maximum FD was found at the 75° blasting angle when the FD was calculated in a direction parallel to the blasting direction. No such peak is found when FD is calculated in a direction perpendicular to grit blasting. The reason for this discrepancy might be a weakness in the robustness of the method or that too small a number of frames was used (18 in each direction for each sample).

The computed average FD of the parallel and perpendicular direction is given in Fig. 11. The FD increased with the blasting angle and reached a maximum of 1.04 at a 75° angle, decreasing slightly at a 90° blasting angle (for the samples sprayed with a 90° angle). This trend was not encountered for samples sprayed with the same angle at which they were grit blasted, where the FD increased continuously up to 90°. There is no reason to believe that there should be any difference between the two curves because it can be assumed that the spray angle will not affect the texture of the interface.

The correlation between the FD and the adhesion strength in Fig. 12 has to be considered as poor (r^2 = 40% and 68%, respectively, for the samples sprayed at the same angle as they had been blasted and the ones sprayed at 90°). A better correlation was found between the adhesion strength and the R_a with an r^2 value higher than 84% (Fig. 13). This suggests that the characterization of the adhesion strength by FD based on a linear in-

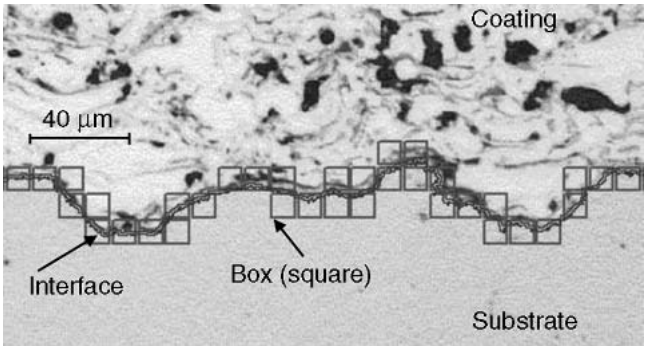

Fig. 7 Typical optical micrograph of a cross section investigated by image analysis and implementing the "Box method"

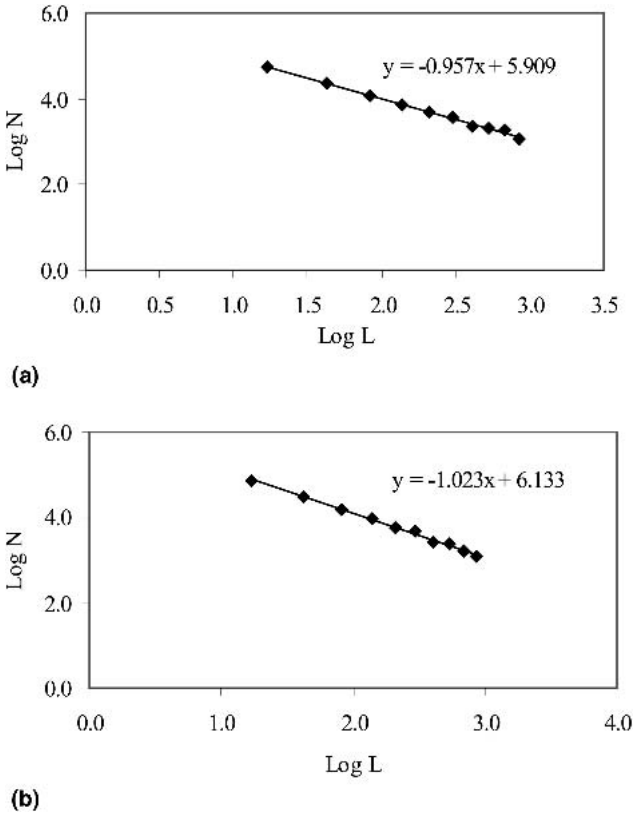

Fig. 8 Fractal characteristic of the blasted surface for different angles. (a) log N-log L plot for the 45°/45° blasting/spraying angle combination; (b) log N-log L plot for the 75°/75° blasting/spraying angle combination

Table 3 Adhesion strength data used for the *t*-test

Blasting/spraying angle combinations	Adhesion strength, MPa					(45°/90° as reference group) *t*-value	(45°/90° as reference group) Probability of nonsignificant difference between two groups, %
45°/90°	19.2	23.1	24.7	23.8	22.4	…	…
55°/55°	19.8	29.1	26.7	26.9	24.8	1.54	16
65°/65°	19.7	26.1	33	27.4	21.7	1.17	28
75°/75°	28.3	28.1	26.8	24.5	24.7	3.09	1.5
90°/90°	24.6	31.6	26.4	27.9	29.6	3.49	0.82

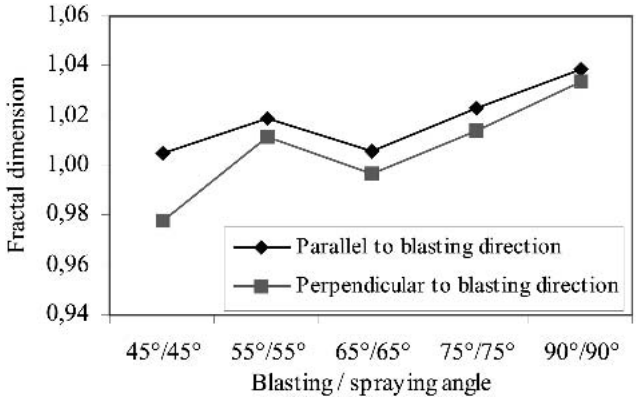

Fig. 9 FD for different grit-blasting/spraying angles

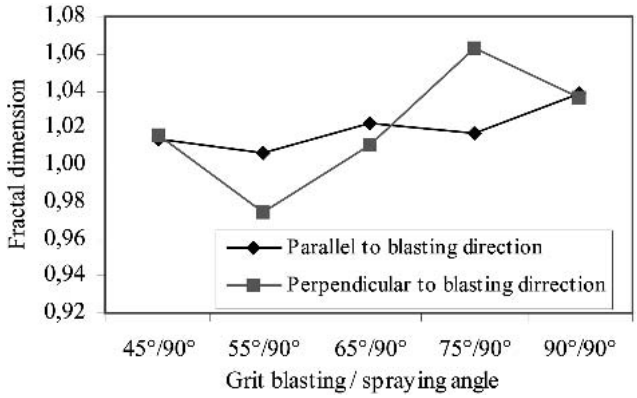

Fig. 10 FDs for different blasting angles and a 90° spraying angle

terface is too simple. A three-dimensional fractal analysis method might be required, such as plane fractal geometry (Ref 13), to characterize the surface topography.

4. Conclusion

From this study several conclusions were obtained:

- The maximum adhesion strength was found to be close to a 90° blasting and spraying angle.
- A maximum shadowing effect was noticed at a 55° blasting angle and a 90° spraying angle.
- An increase in adhesion strength of 15% could be achieved from the commonly used blasting/spraying angle combination of 45°/90° to the 75°/75° combination.
- The different surface characterization parameters that were used for correlation with measured adhesion strength of the coating (R_a and FD) show more and less agreement, respectively. Thus, mechanical cramping of the coating to the substrate surface might be regarded as the primary mechanism of adhesion.
- A line fractal-analysis method based on the cross-section profile interface seems to not be capable of describing the adhesion strength.

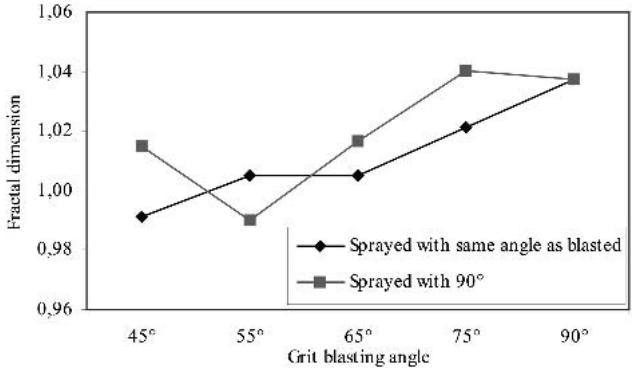

Fig. 11 Average FD for different blasting angles

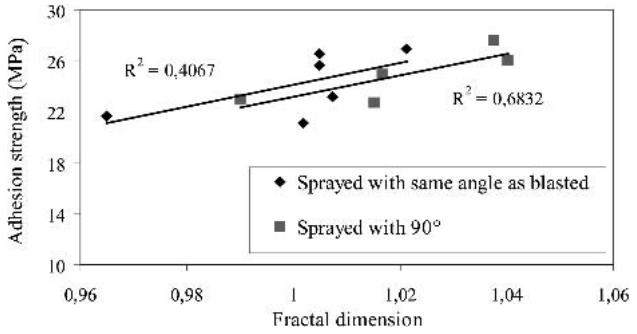

Fig. 12 Adhesion strength versus FD for different angle combinations

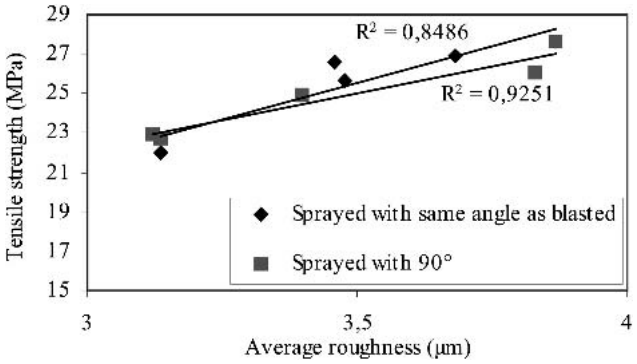

Fig. 13 Adhesion strength versus R_a for different angle combinations

Acknowledgments

The staff at the thermal spray department at Volvo Aero Corporation is gratefully acknowledged for providing all the equipment related to thermal spraying and the SEM equipment, in addition to fruitful discussions. The work was funded by the Foundation for Knowledge and Competence Development and by European Community Structural Funds.

References

1. M. Mellali, A. Grimaud, A.C. Leger, P. Fauchais, and J. Lu, Alumina Grit Blasting Parameters for Surface Preparation in the Plasma Spraying Operation, *J. Thermal Spray Technol.,* Vol 6 (No. 2), 1997, p 217-227

2. D.T. Gawne, B.J. Griffiths, and G. Dong, The Influence of Pretreatment on the Adhesion of Ceramic Coatings on Steel, *Trans. Inst. Metal Finish.,* Vol 75 (No. 6), 1997, p 205-207
3. J. Wigren, Grit Blasting as Surface Preparation Before Plasma Spraying, *Thermal Spray Technology: New Ideas and Processes,* D.L. Houck, Ed., Oct 24-27, 1988 (Cincinnati, OH), ASM International, 1988, p 99-104
4. S. Amada and A. Satoh, Fractal Analysis of Surfaces Roughened by Grit blasting, *J. Adhesion Sci. Technol.,* Vol 14 (No. 1), 2000, p 27-41
5. S.D. Siegmann and C.A. Brown, Investigation of Substrate Roughness in Thermal Spraying by a Scale-Sensitive 3-D Fractal Analysis, *Thermal Spray: Meeting the Challenges of the 21st Century,* C. Coddet, Ed., May 25-29, 1998 (Nice, France), ASM International, 1998, p 831-836
6. S. Siegman, Thun, and C.A. Brown, Surface Texture Correlation with Tensile Adhesive Strength of Thermally Sprayed Coatings using Area-Scale Analysis, *Tagungsband Conference Proceedings,* E. Lugscheider and R.A Kammer, Ed., DVS Deutscher Verband für Schweißen, 1999, p 355-360
7. "Standard for Surface Roughness Measurements," VAC: PST347, Volvo Aero Corporation, 1987
8. "Standard for Grit Blasting Determination by X-ray Fluorescence," Instruction A-37 Reg. No. 9340-93-231, Volvo Aero Corporation
9. S.O. Stalberg, Method for Preparation of Test Bodies, European Patent 1071553, 2002
10. Metallographic Preparation Procedure, VAC: O-915391231, Volvo Aero Corporation
11. "Standard Test Method for Adhesion or Cohesion Strength of Thermal Spray Coatings," C 633-01, *Annual Book of ASTM Standards,* ASTM, 2001, p 1-7
12. R. Christensen, *Analysis of Variance, Design and Regression: Applied Statistical Methods,* Chapman & Hall, 1996, p 30-31
13. S. Amada and T. Hirose, Application of Plane Fractal Geometry to Adhesion Strength of Thermal Sprayed Coatings, *Thermal Spray: Surface Engineering via Applied Research,* C.C. Berndt, Ed., May 8-11, 2000 (Montréal, Quebec, Canada), ASM International, 2000, p 1071-1076